International Journal of Research Studies in Science, Engineering and Technology
Volume 4, Issue 8, 2017, PP 10-19
ISSN : 2349-476X

Evaluation of Kinetic Profile of Release of Tetracycline from Microparticles of Alginate-Chitosan Hydrogels

Mônica Huguenin de Araujo Faria[1]*, Letícia Paifer Marques[1], Amanda Caroline Inácio de Almeida[1], Gabriela Souza Bezerra[1], Eduardo Santana da Silva[1], Francisco Benedito Teixeira Pessine[1]

Institute of Chemistry, State University of Campinas, Campinas, Brazil

***Corresponding Author:** Mônica Huguenin de Araujo Faria, Institute of Chemistry, State University of Campinas, Campinas, Brazil, e-mail: professora.quimica@yahoo.com.br*

Received Date: 30-10-2017 ***Accepted Date: 09-11-2017*** ***Published Date: 16-11-2017***

ABSTRACT

This paper describes the production and characterization of biodegradable polymeric microparticles containing the tetracycline hydrochloride antibiotic for oral administration. Chitosan and sodium alginate, both polyelectrolytes, were used to prepare microparticles whose network is an interpenetrating network (IPN) type network. Sodium alginate was cross-linked by calcium ions to control the release of tetracycline. The characterizations were performed by FTIR, TGA and size distribution. The kinetic release profiles were evaluated in simulated gastric fluid. The influence of the amount of each component on the characteristics of the microparticles and the kinetics of the release of tetracycline in the simulated gastric fluid was also evaluated. The results show a minimization of the effect of the explosion in simulated gastric fluid. A sustained release profile was observed over the period of time evaluated. FTIR results suggest that there are differences in the types of interactions between the reagents and tetracycline. These differences had an influence on the launch profiles.

Keywords: *alginate, chitosan, drug delivery system, tetracycline, polyelectrolytes*

INTRODUCTION

One of the problems with antibiotic administration is the poor adherence of patients undergoing prolonged treatment, leading to a discontinuation of antibiotics before the end of treatment. This has contributed to increase bacterial resistances, making it difficult to treat common diseases such as syphilis. This is one of the reasons justifying the development of sustained release devices with non-toxic and biodegradable materials for drug delivery. These devices, by releasing the drug over a long period of time, ensure that the patient receives continuous doses throughout the treatment period [1].

Such devices may be prepared from various materials, such as hydrogels, for example. Hydrogels based on natural polymers, such as alginate and chitosan, are used as reagents of sustained release drug delivery devices. Chitosan is a naturally occurring biodegradable and biocompatible linear polymer composed of D-glucosamine and N-acetyl-D-glucosamine units [2]. It is obtained by the deacetylation of chitin and is used in many biomaterials. Chitosan improves the gastric residence time of a drug delivery system due to the presence of D-glucosamine units and, in the cationic form, has mucoadhesive properties [3]. Alginate is also a naturally occurring straight chain polysaccharide. That is, a biopolymer constituted by monomers of β–D-manuronic and α-L-guluronic acids that can be obtained from brown algae. It has carboxylic groups through which the polymer network interacts with calcium ions and forms a self-organized structure by cross-linking the alginate chains. [1].

Due to their properties, alginate and chitosan were used in the development of various devices to transport drugs, cells, enzymes, DNA, etc. Chitosan and alginate are polyelectrolytes and, when putted together, may constitute a polyelectrolyte complex (PEC). When chitosan is physically mixed with alginate crosslinked by calcium ions, they form a hydrogel of interpenetrating network (IPN) with the ability to swell, thus promoting drug release [4].

One of the most common problems of drug delivery devices is the explosive (burst) effect,

in which much of the drug is released at the onset of the release, as the microparticles (MP) have pores which allows a fast release of the contained drug. This effect leads to the release of large amounts of drug in the body, surpassing the terapeutic levels [6].

In this paper, we present a low-cost water-based system without toxic solvents to prepare MP of chitosan and alginate. Aside from the fact that these water-insoluble microparticles prevent the burst effect. This methodology is based on the increased degree of cross-linking of alginate's network which slows down the drug release [1].

Tetracycline hydrochloride is a broad spectrum antibiotic [4, 20]. It acts on gram-negative and gram-positive bacterias and has been used to treat many infections, such as gonorrhea, a genitourinary tract infection caused by *N. gonorrhoeae*, pharyngitis, pneumonia, otitis and sinusitis caused by *H. influenzae*. It can be used for treatment of actinomycosis and skin infections caused by *S. aureus* and syphilis and urinary tract infections caused by *Klebsiella* and *Escherinchia*, respectively [5]. The usual dosage is 500 mg capsules of oral administration every six hours. One of the advantages of producing antibiotic-containing microparticles is to avoid or decrease their adverse/colateral side effects, as well as the possible interaction of this drug with other medications or foods. In addition, it also has the capability to maintain the therapeutic dose during long-term treatments. In syphilis treatment, for example, which may last from 15 to 30 days, the formulation containing microparticles may be used to administer the antibiotic directly at the site of infection. Therefore, a therapeutic dosage of the drug can be maintained only around the active area. Another advantage of the use of drug delivery systems is to decrease the amount of drug distributed systemically in the body [4].

MATERIALS AND METHODS

Chitosan* (CH) (Chitopharm S) was provided by Cognis Brazil (MW 300kDa, 83% deacetylated), sodium alginate* (SA) (Manugel LBA) was provided by ISP (MW 79kDa, 0,71 M/G (Manuronic/Guluronic). Glacial acetic acid P.A. (Labsynth), hydrochloric acid P.A. 37% (Labsynth), calcium chloride P.A. (Labsynth), sodium chloride P.A. (Labsynth), tetracycline hydrochloride (TC) (Sigma Aldrich), phosphoric acid (Labsynth), acetonitrile HPLC grade (J.T. Baker), pepsin (Acros Organics), dialysis cellulose membrane (typical molecular weight cut-off 12 to 16kDa - InLab).

*These properties were determined by methods of instrumental analysis, cited in the work of Barboza (2013) [14].

Preparation of Microparticles

In previous work of our research group (Barboza, 2013 [14]) different methodologies used to prepare microparticles with alginate and chitosan were compared, showing that the preparation by mechanical shearing with Ultra-Turrax® with a single step addittion of each reagent produced particles with smaller diameters and higher loading capacity (LC) and entrapment efficiency (EE) (**Figure 1)**.

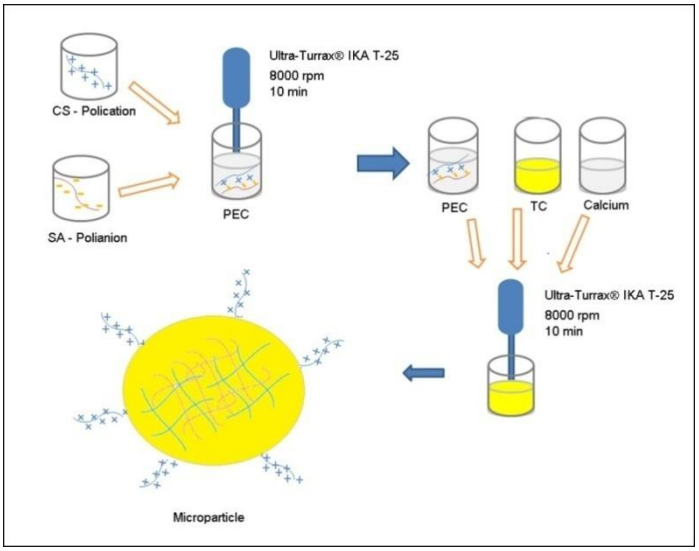

Figure1. *Scheme of preparation of microparticle of alginate-chitosan loaded with tetracycline.*

Influence of formulation components

A 2^3 experimental design with a central point was used to evaluate the influence of each component on some characteristics of the formulation containing microparticles, such as diameter, EE, LC and mass of TC released (**Tables 2 and 3**). Central point was prepared in duplicate. The total biopolymer mass, the volume of the suspensions, and the conditions of preparation were fixed.

Table1. *Level of factors used in the experimental design*

Factor/level	-1	0	+1
F1	1:2	1:1	2:1
F2	1:2	1:1	2:1
F3(mg)	50	100	150

F1: Ratio between amounts of CH and SA; F2: Ratio between amounts of SA and $CaCl_2$; F3: Ratio between amounts of total polymer and TC.

Table2. *2^3 experimental design with a central point*

Experiment	F1	F2	F3
PL01	+	+	+
PL02	-	+	+
PL03	+	-	+
PL04	-	-	+
PL05	+	+	-
PL06	-	+	-
PL07	+	-	-
PL08	-	-	-
CP	**0**	**0**	**0**

Microparticles Characterization

Size Distribuition

The microparticles size distribution, expressed as volume frequency, was determined with the Malvern Mastersize 2000 APA 2000 Hydro 2000s AWA2001 equipment. Measurements were transformed by the equipment's software in number of particles, in order to minimize the effect of particles whose diameter is much larger.

Entrapment Efficiency And Loading Capacity

To determine the values of EE and LC of TC in microparticles, 500 µL of each sample were transferred to an Amicon Ultra Ultrafiltration Device 0.5 MWCO 100k and centrifuged at 10,000 rpm for 10 minutes. The TC concentration was determined by reverse phase HPLC using a Waters ACQUITY System with a variable wavelength detector (Waters ACQUITY V) set at 280nm, a C18 column Zorbax XDB (250mm x 4,6 mm, 5 µm) (Agilent) at 50°C and a injector fitted with a 10µL loop. The mobile phase consisted of acetonitrile/phosphoric acid 0.1% (15:85, v/v) delivered at a flow rate of 1mL/min.

The analytical curve was obtained in the range of 0.20 to 2.0 µg of TC. The amount of TC in the total microparticles was calculated using a calibration curve method (USP 30 – NF 25, 2007 and HUSSIEN, 2014 [21]). EE and LC were calculated with **Equation 1** and **Equation 2**, respectively.

$$EE\ (\%) = \frac{(\text{Total TC mass} - \text{free TC mass})}{(\text{total TC mass})} \times 100$$

Equation 1

$$LC\ (\%) = \frac{(\text{Total TC mass} - \text{free TC mass})}{(\text{total polymer mass})} \times 100$$

Equation 2

Compatibility of Tetraciclyne with Excipients

The drug-polymer interactions in the microparticles were evaluated by Fourier transform infrared (FTIR) spectra, recorded with an Agilent Cary spectrophotometer, model 630 FTIR. FTIR data was collected in the medium infrared region (4000-400cm^{-1}) using the attenuated total reflection (ATR) sampling mode. Samples were placed directly on the surface of the ATR crystal. The FTIR spectra registered for samples of TC, CH, SA, microparticles loaded with TC, and also for physical mixture of the polymers.

Thermal Analysis

Differential scanning calorimetry (DSC) was used to analyse the entrapment of TC inside the microparticles using a DSC thermal analyzer TA Instruments, model 2910 at a heating rate of 10°C per minute in the range of 30 to 250°C with an nitrogen atmosphere at a flow rate of 50 mL/min. DSC thermograms were recorded for TC and for microparticles loaded with TC. Samples had been dried before the experiment in a drying oven for 24 h at 50°C.

In Vitro Release Study

In vitro release of TC from the microparticles was performed using a Membrane Isolation-Assay (MI-A) method (continued method / Dialysis bag method) [7]. This study was performed in simulated gastric fluid (SGF, 0.1 M HCl, pH 1.2). An aliquot of 8 mL of the microparticle suspension was centrifuged. Supernatant was discarded and replaced with 8 mL of SGF. Suspension was placed into a

dialysis bag that was sealed and immersed into a beaker containing 100 mL of SGF. The entire system was kept at 37°C under continuous magnetic stirring. Aliquots of 1 mL of the receiver media were withdrawn, successively, at defined times. Fresh media was used to maintain the total volume constant. SGF assay was performed for 2 hours, the mean time of digestion in the human stomach. Samples were filtered using a 0.45µm filter and drug content was determined as already described (item 2.2.2). In order to understand the release mechanism of the drug from the microparticles, data were fitted to various kinetic models. The best one was chosen by its correlation coefficient (R^2). The different models applied for the drug release data were zero order, first order, Higuchi's and Korsmeyer-Peppa's model [7 – 12].

Zero order

$$\frac{M_t}{M_\infty} = k_0 t \qquad \textbf{Equation 3}$$

where M_t is the amount of drug released in time (t), M_0 is the initial amount of drug in the microparticles and k_0 is the release kinetic constant.

First order

$$M_t = M_0\, e^{-K_1 t} \qquad \textbf{Equation 4}$$

where M_t is the amount of drug released in time (t), M_0 s the initial amount of drug in the microparticles and k_1 is the release kinetic constant.

Higuchi

$$M_t - M_0 = K_h \cdot t^{1/2} \qquad \textbf{Equation 5}$$

where M_t is the amount of drug released in time (t), K_H is the release kinetic constant.

Korsmeyer-Peppas

$$\frac{Mt}{M\infty} = k_{PK}\, t^n \qquad \textbf{Equation 6}$$

Where M_t is the amount of drug released in time (t) and M_∞ is infinity time. K_{PK} accumulates in itself the structural and geometric characteristics of the microparticle

Results and Discussions

Microparticles Size Distribution

Figure 2 shows that the size distribution is monomodal.

The different samples obtained with the experimental design contain microparticles with a diameter distribution around 5 µm (**Figure 3**) and similar polydispersity index (PDI) (**Table 3**).

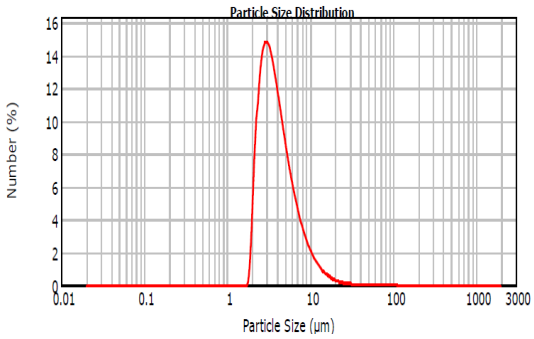

Figure2. *Particle size distribution of CP microparticle*

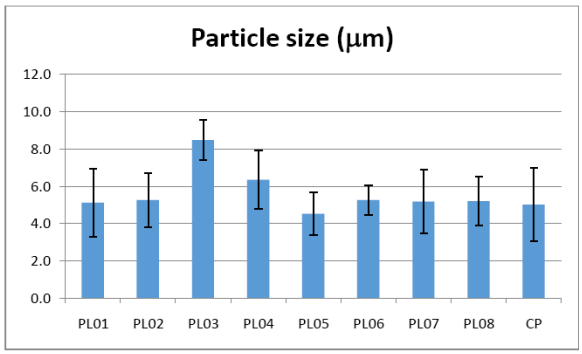

Figure3. *Particle size of microparticles*

Table3. *Average diameter and polydispersity index of microparticles*

Sample	Particle diameter (µm)*	PDI
PL01	5.1±1.8	1.3
PL02	5.2±1.5	1.5
PL03	8.5±1.1	1.1
PL04	6.3±1.6	1.2
PL05	4.5±1.2	1.4
PL06	5.3±0.8	1.8
PL07	5.2±1.7	1.6
PL08	5.2±1.3	1.7
CP	5.0±2.0	1.5

Mean value ± S.D., n = 3

Entrapment Efficiency and Loading Capacity

The values of EE and LC are shown in **Table 4** and **Figures 4** and **5**.

Table4. *Entrapment efficiency and loading capacity of microparticles*

Sample	LC (%)*	EE (%)*
PL01	83.9±1.2	83.9±1.2
PL02	85.5±1.5	85.5±1.5
PL03	85.6±3.7	85.6±3.7
PL04	86.6±2.8	86.6±2.8
PL05	19.0±6.0	56.9±18.0
PL06	23.1±3.1	69.2±9.2
PL07	20.4±2.3	61.1±6.9
PL08	23.4±2.8	70.3±8.5
CP	52.7±4.1	82.8±6.5

Mean value ± S.D., n = 3

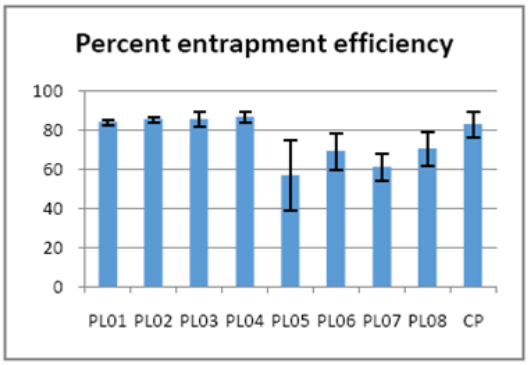

Figure4. *Loading capacity of MP*

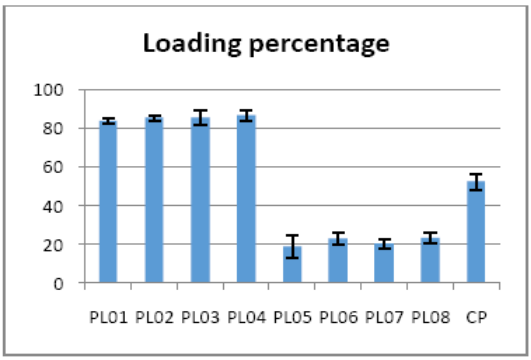

Figure5. *Entrapment efficiency of MP*

Influence of the Components

Table 5 shows entrapment efficiency (EE), loading capacity (LC), andaverage particles diameter (D). **Table 6** shows the effects of the variations in the amounts of reagents (factors) on the characteristics of MPs (responses) and the results of adjustments with a linear model.

Table 5: *LC, EE and average particle diameter* **(D)**

Sample	LC (%)	EE (%)	D (μm)
PL01	83.9±1.2	83.9±1.2	5.1±1.8
PL02	85.5±1.5	85.5±1.5	5.2±1.5
PL03	85.6±3.7	85.6±3.7	8.5±1.1
PL04	86.6±2.8	86.6±2.8	6.3±1.6
PL05	19.0±6.0	56.9±18.0	4.5±1.2
PL06	23.1±3.1	69.2±9.2	5.3±0.8
PL07	20.4±2.3	61.1±6.9	5.2±1.7
PL08	23.4±2.8	70.3±8.5	5.2±1.3
CP	52.7±4.1	82.8±6.5	5.0±2.0

Table6. *Results of the experimental design and of the adjustment of release experiments data to a linear model.*

Results	Factor	R^2	CRL	SD	*p*	-95%	+95%
EE (%)	Intercept		76.8	1.9	0.0000	73.1	80.6
	F1	89.2	6.0	4.5	0.2760	-2.9	14.9
	F2		2.0	4.5	0.6822	-6.8	10.9
LC (%)	Intercept		53.1	0.5	0.0000	52.1	54.1
	F1	99.9	2.4	1.2	0.1257	0.2	4.7
	F2		1.2	1.2	0.3868	-1.1	3.4
Diameter	Intercept		5.2	0.3	0.0001	4.6	5.9
	F1		-0.3	0.8	0.7506	-1.9	1.3
	F2	49.3	0.7	0.8	0.4735	-1.0	2.3

R^2 *indicates the adjustment of data to the model,* ***CRL*** *is the coefficient for each factor,* ***SD*** *is the standard error,* ***p*** *is the parameter of significance in the equation with 95% of confidence, the columns* ***- 95%*** *and* ***+ 95%*** *indicate the confidence interval.*

The parameters described in **Table 3** indicate a poor level fitting the linear model for the particle size data, since R^2 was 49.3%. However, there was a good adjustment of the linear model for other parameters, since R^2 ranged from 89.9 and 99.9%. The choice of factors that really influenced the characteristics of MP was based on the p-value obtained for each factor. If the *p*-value was ≤0.05 the factor would be considered significant [12].

Linear models (**Equations 2 and 3**) that represent the influence of the amount of reagents (**Table 3**) on MP characteristics were obtained using the spreadsheet developed by Teofilo & Ferreira (2005).

$EE(\%) = 76.8(\pm 1.9) - 21.4(\pm 4.5).TC$ **Equation 7**

$LC(\%) = 53.1(\pm 0.5) - 64(\pm 1.2).TC$ **Equation 8**

Linear models obtained for EE and for LC were based only in the significant factors. However, it was found that a suitable linear model (R^2 = 49.3%) was not obtained for the particle size, since no factor was significant ($p > 0.05$). Despite this, the drug/polymer ratio, whose p = 0.2, although being higher than the significance level, suggests that there is some influence of the TC amount on particle size, as also observed by BARBOZA (2010) [14]. In contrast, CALADO, ROSSI & ROCHA-LEÃO (2013) [15] by preparing particles with the same mechanical shear method, observed that increasing the degree of crosslinking of the particle decreases particle size [2, 14, 15].

Entrapment efficiency was shown to be independent of the polymers mass and of the SA/calcium ratio and dependent on the TC mass. This result suggests that it is possible to obtain higher values of EE in preparations with higher amounts of TC. Similar fact was observed by Takka and Gürel (2010) [13]. Analysis of the non-significant factors suggests that the CH/SA ratio, whose p = 0.2760, has some influence on the entrapment efficiency. This may be justified by the competition between the positive sites of TC and CH and the negative sites of SA chains [13, 14].

Loading capacity has been shown to be dependent only on TC mass. In all models, the negative signal obtained for the TC coefficient

in the linear model indicates that the loading capacity decreases as the TC mass increases [14]. Note that the CH/SA ratio and the SA/Calcium ratio are not part of the linear models because they are not significant factors. Nevertheless, their low values of p ($p \cong 0.1$) suggest that both the CH/SA ratio and the SA/Calcium ratio have some influence on the percentage of TC loading [14, 16].

3.4. Thermal Analysis

DSC thermograms obtained are shown in **Figure 6.** DSC results show that SA and CH exhibit endothermic events at 96.11°C and at 66.50°C, respectively. Drug termogram show a sharp exothermic peak at 231.58°C corresponding to its thermal degradation. These exothermic peaks were present in the thermograms obtained for PL01, PL02, PL03, PL04 and CP formulations (**Figure 6**). DSC thermograms obtained for the other samples (PL05 to PL08) (**Figure 6**) did not show the tetracycline degradation peak, indicating that this drug was likely dissolved in the matrix formers and/or dispersed in the amorphous particles. The addition of diferent amounts of the crosslinking agent (calcium ions) did not substantially change the thermograms of the samples.

Endothermic events reveal the relationship between transposition and fusion of the polymer chain. Melting point values obtained for the microparticles samples were intermediate between those observed for SA (129.24°C) and CH (114.35°C). However, the decomposition values obtained for TC in the samples PL01, PL02, PL03 and PL04 were lower than those observed for pure drug (231.58°C), indicating a lower stability of the drug in these formulations. However, in the thermograms obtained for samples PL05, PL06, PL07, PL08 and CP there are no exothermic events indicating that in these preparations there is no decomposition of CT, suggesting that these samples provide higher thermal stability for the drug [14].

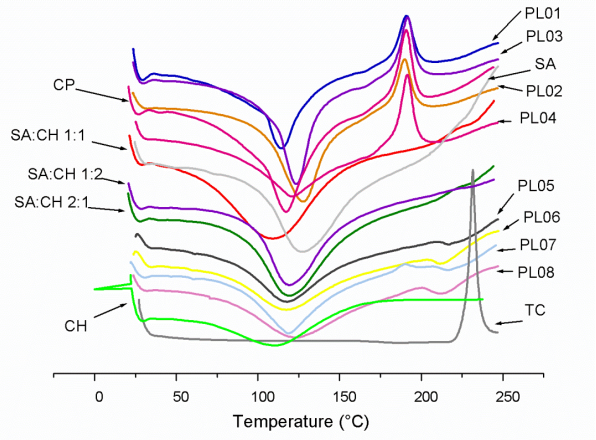

Figure6. *DSC thermograms obtained for SA, CH, TC and microparticles samples*

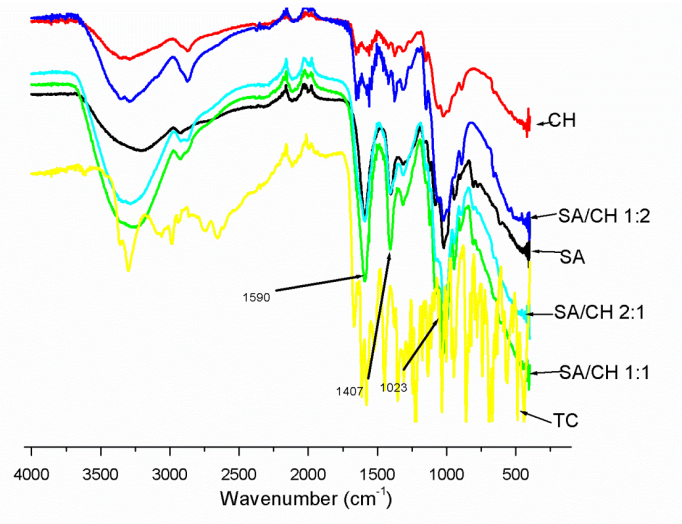

Figure7. *FTIR spectra of SA, CH, TC and physical mixture physical mixtures of SA and CH in rations of (1:1), (1:2), and (2:1).*

Compatibility of Tetraciclyne with the Excipients

In order to elucidate and differentiate the interactions between SA and CH, the spectra of their physical mixture, in the same proportion as those present in MP samples, was obtained. In **Figure 7** and **Table 7** are the bands assignment for these spectra one can note that the band 1590 cm^{-1} and 1407 cm^{-1} related to the carboxyl group (COO^-) is present in both (1:1) and (2:1) mixtures spectra, indicating interactions between the carboxylate negative charges of SA and the amonium positive charges of CH. This band is absent in the (1:2) mixture spectra, but the band 1560 cm^{-1} related to the amine group (NH_2) of CH is present in this mixture. The presence of these bands suggests that there are free amino groups in SA/CH 1:2.

Table7. *Bands of the main groups*

Group	Band (cm^{-1})
νO-H	3600-3200
νC-H alifatic Csp^3	2960-2720
δCOO^-	1630-1550
δN-H	1580-1495
δCH_3	1390-1370
νC-N	1360-1080
νC-O	1275-1020

Reactants spectral bands, with some shifts and/or attenuations, are also present in the drug loaded microparticles spectra (**Figure 8**).

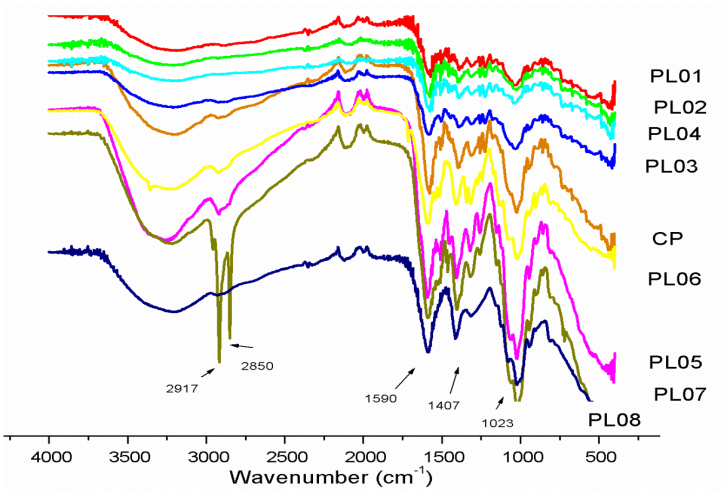

Figure8. *FTIR spectra of PL01 – PL08 and PC microparticles*

Analysis of the bands corresponding to the major functional groups of the reactants in each microparticle spectra (**Figure 8**) indicate if there are interactions between such groups, or not. In addition, knowing the degree of interaction of these groups it is possible to elucidate phenomena such as greater or lesser TC incorporation and the higher or lower rate of TC releases in the SGF release assays.

Spectra in **Figure 8** shows that in the group of microparticles with the greatest amount of drug (PL01 to PL04) the characteristic band of the carboxyl groups (COO^-) of the SA (1590 cm^{-1} and 1407 cm^{-1}). The characteristic bands of the carboxyl group and of the amino group of the CH, and the characteristic band of the amide group of the TC are all less intense than those in the spectra of the sample group with the lower amount of drug (PL05 to PL06 and PC, as in **Figure 8**). This result suggests that the microparticles with greater amount of TC have a greater degree of interactions between the functional groups of their components than the microparticles with less amount of drug, showing that the tetracycline functional groups also interact with the groups of the polymer matrix.

In Vitro Dissolution Study

Different release profiles were observed for each sample. The data represents the mean ± SD of each experiment performed in duplicate. The graph obtained is shown in **Figures 9 and 10**.

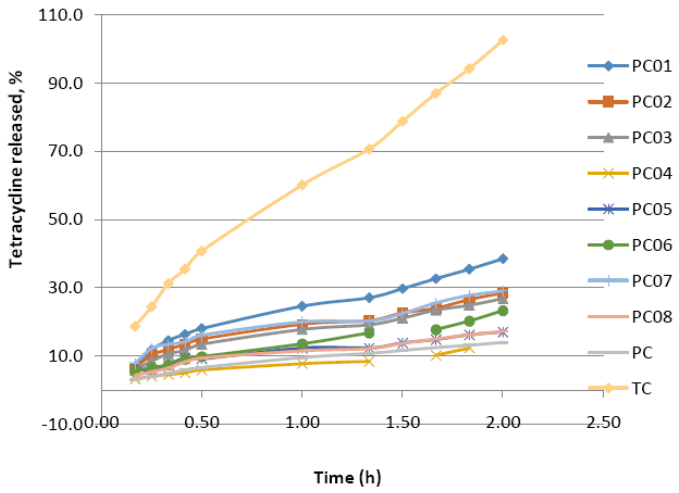

Figure9. *Release profile in simulated gastric fluid of each MP sample and free TC.*

The release profile curves obtained until up 60% of the release experiment were characterized by zero order, first order, Higuchi's, and Korsmeyer-Peppas models. The evaluation of the better adjustment of the release profile curve to the kinetic model was done considering the highest R^2 value (**Table 8**).

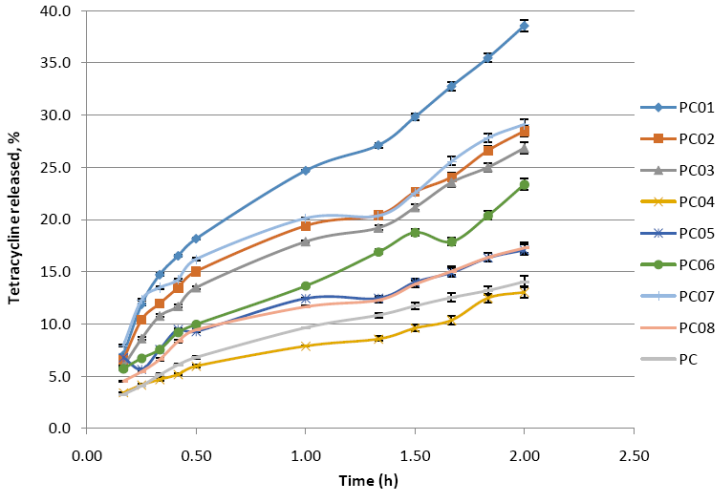

Figure10. *Expanded view of the release profile curves of release profile in simulated gastric fluid of each MP sample.*

In the Korsmeyer-Peppas model, the coefficient n is related to the type of matrix and informs the mechanism of drug release from the SLF [10, 11]. For values of n equals to 0.43 the drug transport is due to Fickian diffusion. For n values between 0.43 and 0.85 the drug release occurs through an anomalous transport and for values of n equals to 0.85 the transport occurs by swelling. The obtained n values for all release curves were in between 0.43 and 0.85 (**Table 8**), suggesting that the release kinetic of the samples were of the anomalous [10, 11, 12].

Table8. *R^2 of kinetic models for the release profile curves of TC in SGF*

Sample	Zero Order	First order	Higuchi	Korsmeyers-Peppas	n
PL01	0.9759	0.6684	0.9961	0.9481	0.69
PL02	0.9554	0.6814	0.9928	0.99	0.59
PL03	0.9775	0.7126	0.9969	0.9976	0.61
PL04	0.9756	0.9043	0.9752	0.9765	0.52
PL05	0.9701	0.8692	0.9793	0.9781	0.48
PL06	0.9586	0.8858	0.9735	0.9578	0.60
PL07	0.9247	0.7853	0.9555	0.9550	0.53
PL08	0.9533	0.8502	0.9799	0.9800	0.56
CP	0.9813	0.8753	0.9990	0.9984	0.66

However, since the TC release profile from PL01, PL02, PL05, PL06 and PL07 fit better to the Higuchi model, it is suggested that in these samples the release occurs mainly by diffusion [8, 9, 10, 11].

Considering the time of the release study in SGF and that, at the end of that time, most of the particles released about 20% of the total amount of encapsulated TC., Whereas in the same period, the free TC was 100% released, so the microparticles promoted a sustained release and their use might have minimized the adverse gastric side effects caused by TC oral administration.

When comparing the TC release profiles of PL01 and PL04 samples, it was observed that PL04 released a higher amount of TC than PL01. This phenomenon can be justified due to their composition. PL04 sample has a higher amount of SA and calcium than PL01. Nevertheless, the degree of crosslinking of the SA network in PL04 must be higher than the one of the polymer network in PL01.

CONCLUSIONS

The characterization indicated that there are different types of interaction between SA, CH and TC in each sample. Thermal analysis indicated that the preparations have lower thermal stability than pure reagents. This is not necessarily negative, since the microparticle formulations would be used at human body temperature, 37^{o}C.

The differences in the interactions of the reactants with each other and with TC influenced both loading capacity and encapsulation efficiency, as well as the release profiles, since the interaction of TC and matrix was different in all MP samples.

FTIR results indicated that TC interacts with the polymer matrix, and this is one of the reasons why the drug is not easily released in the *in vitro* release assays, avoiding the occurrence of the burst effect.

The disappearance of the exothermic peak related to the drug on some MP samples thermograms (PL05, PL06, PL07 and PL08) reflect the complete entrapment and the miscibility or dispersion of the drug in the polymer matrix. Also, the presence of this peak on other thermograms (PL01, PL02, PL04 and PC) suggests that part of the drug is not dispersed in the particle, it is crystallized instead.

CONFLICTS OF INTEREST

None

ACKNOWLEDGEMENTS

The authors acknowledge the Federal University of Rio de Janeiro (UFRJ) and the State University of Campinas (Unicamp) for the technical support needed to carry out this work.

REFERENCES

[1] I. Chopra, M. Roberts, Tetracycline Antibiotics: Mode of Action, Applications, Molecular Biology, and Epidemiology of Bacterial Resistance. Microbiol. Mol. Biol. Rev. (2001), 65(2) 232-260. Doi: 10.1128/MMBR.65.2.232-260. 2001

[2] M. Sanchita, K. S. Senthil, K. Balakrishnam, B. S. Kumar, Development and evaluation of calcium alginate beads prepared by sequential and simultaneous methods. Brazilian Journal of Pharmaceutical Sciences. (2010), 46(4), 785-793. DOI: https://dx.doi.org/10.1590/S1984-82502010000400021.

[3] L.A. Caetano, L. Figueiredo, A. J. Almeida, L. M. D. Gonçalves, BCG-loaded chitosan microparticles: Interaction with macrophages and preliminary in vivo studies, J. Microencapsul., (2017), 34(2):203-217. DOI: 10.1080/ 02652048. 2017.1316325.

[4] L. Wang, E. Khor, L-Y. Lim, Chitosan-Alginate-$CaCl_2$ System for Membrane Coat Application. American Pharmaceutical Association J Pharm Sci, (2001) 90:1134–1142. DOI: http://dx.doi.org/ 10.1002/jps.1067.

[5] A. Alok, N.K. Chaudhury, Tetracycline hydrochloride: A potential clinical drug for radioprotection. Chem. Biol. Interact., (2016), 245:90-9. DOI: 10.1016/j.cbi.2016.01.001.

[6] N. A. Buckley, A. H. Dawson, D. A. Reith, Controlled Release Drugs in Overdose: Clinical Considerations. Drug-Safety, (1995), 12: 73-84. DOI: https://doi.org/10.2165/00002018-199512010-00006

[7] Y. Zhou, C. He, K. Chen, J. Ni, Y. Cai, X. Guo, X. Y. Wu, A New Method for Evaluating Actual Drug Release Kinetics of Nanoparticles inside Dialysis Devices via Numerical Deconvolution, Journal of Controlled Release. (2016), 243(1):11-20. DOI: https://doi.org/10.1016/j.jconrel.2016. 09.031.

[8] J. Siepmann, F. Siepmann. Mathematical modeling of drug delivery. Int J Pharm.(2008). Int J Pharm 364(2): 328-343. DOI: 10.1016/ j.ijpharm.2008.09.004

[9] P. Costa, J. M. S. Lobo, Modeling and comparison of dissolution profiles. European

Journal of Pharmaceutical Sciences, (2001), 13 (2): 123-133, DOI: https://doi.org/10.1016/S0928-0987(01)00095-1.

[10] Siepmann, J., Peppas, N. A. Modelling of drug release from delivery systems based on hydroxypropyl methylcellulose (HPMC). Advanced Drug Delivery Reviews (2001), 48(2-3): 139-157. DOI: https://doi.org/10.1016/S0169-409X (01)00112-0

[11] J. Siepmann, N.A. Peppas, Higuchi equation: Derivation, applications, use and misuse. Int J Pharm, (2011), 418(1):6-12. DOI: 10.1016/ j.ijpharm.2011.03.051.

[12] B. Barros Neto, I.S. Scarmínio, R.E. Bruns, Como fazer experimentos: pesquisa e desenvolvimento na ciência e indústria". Third ed., Unicamp, Campinas, 2007.

[13] S. Takka, A. GÜREL, Evaluation of chitosan/ alginate beads using experimental design: formulation and in vitro characterization. AAPS PharmSciTech, (2010), 11(1): 460-464. DOI: 10.1208/s12249-010-9406-z.

[14] A. C. R. N. Barboza, Liberação sustentada do antisséptico clorexidina em micropartículas de quitosana e alginato (doctoral thesis). Campinas, SP: [s.n.], 2013. http://repositorio.unicamp.br/ bitstream/REPOSIP/250355/1/Barboza_AnaClaudiaRuedaNery_D.pdf (accessed 05 September 2017).

[15] V.M.A. Calado, A.M. Rossi, M.H.M. ROCHA-LEÃO, Characterization of Antibiotic-Loaded Alginate-Osa Starch Microbeads Produced by Ionotropic Pregelation. BioMed Research International (2013), 2013(1-11). DOI: http://dx.doi.org/10.1155/2013/472626.

[16] N. Patel, J. Desai, P. Kumar, H. P. Thakkar. Development and In-Vitro Characterization of Capecitabine Loaded Alginate-Pectinate Chitosan Beads for Colon Targeting. Journal of Macromolecular Science, Part B, (2016), 55(1): 33-54. DOI: http://dx.doi.org/10.1080/ 00222348. 2015.1110551.

[17] DYER, B. Aplicações da espectroscopia de absorção aos compostos orgânicos, Ed. Edgard Blücher,São Paulo, 1969.

[18] P. LI, Y-N Dai, J-P Zhang, A-Q Wang, Q.Wei, Chitosan-Alginate Nanoparticles as a Novel Drug Delivery System for Nifedipine. Int J Biomed Sci, (2008), 4(3), 221–228.

[19] K. Mladenovska, et al., 5-ASA loaded chitosan–Ca–alginate microparticles: Preparation and physicochemical characterization. Int J Pharm (2007), 10;345 (1-2): 59-69. DOI: 10.1016/ j.ijpharm.2007.05.059

[20] P. Pniamlang, T. Tongrain, P. Ekabutr, P. Chuysinuan, P. Supaphol, Preparation, characterization and biocompatibility of poly (vinyl alcohol) films containing tetracycline hydrochloride-loaded quaternized chitosan nanoparticles, Journal of Drug Delivery Science and Technology, (2017), (38) 36e44. DOI: https://doi.org/10.1016/j.jddst.2016.12.006

[21] E. M. Hussien, HPLC method validation for modernization of the tetracycline hydrochloride capsule USP monograph. Bulletin of Faculty of Phamacy, Cairo University,(2014), 52 (2): 239-244. DOI: https://doi.org/10.1016/j.bfopcu.2014. 08.002

Citation: *Faria, M.H.A., Marques, L.P., Almeida, A.C.I., Bezerra, G.S., Silva, E.S. And Pessine, F.B.T., "Evaluation of Kinetic Profile of Release of Tetracycline from Microparticles of Alginate-Chitosan Hydrogels", International Journal of Research Studies in Science, Engineering and Technology, vol. 4, no. 8, pp. 10-19, 2017.*